

Isotope Shifts of K X Rays and Variations of Nuclear Charge Radii*

R. B. CHESLER AND F. BOEHM

California Institute of Technology, Pasadena, California

(Received 4 October 1967)

The electronic $K\alpha_1$ isotope shifts have been studied for the following sets of isotopes: $\text{Sn}^{116-124}$, $\text{Nd}^{144-150}$, $\text{Sm}^{148-154}$, $\text{Gd}^{155-158-160}$, $\text{W}^{182-184-186}$, $\text{Hg}^{200-204}$, and $\text{Pb}^{206-208}$. With the help of a curved-crystal spectrometer in the Cauchois geometry the relative wavelengths of fluorescently excited x rays for two enriched isotope samples were measured to a precision of 10^{-7} . The observed shifts, corrected for the normal and specific mass shifts, were compared with calculated shifts, taking into account the volume effect (adjusted for the dynamic quadrupole interaction), screening by the transition electron, and a term arising from the anomalous magnetic moment. The anomalies previously observed in the optical and muonic shifts are established with good accuracy by the present experiments.

1. INTRODUCTION

THE isotope shifts of electronic energy levels reflect the fine variations of the mean-square nuclear charge radius when neutrons are added to the nucleus. These shifts, therefore, can provide information on the detailed changes of nuclear structure. Among the electronic states the K level, lying closest to the nucleus, is particularly appropriate as a nuclear probe. The $K\alpha_1$ x-ray shift gives the K level isotope shift directly since the corresponding L_{III} level shift is negligibly small. As compared to optical transitions, the use of K x rays has the advantage of considerably lesser uncertainties in the evaluation of the experimental observations. In particular, in the case of $K\alpha_1$ x rays for $Z \gtrsim 35$, the screening and mass shift corrections can be accurately estimated.

The first measurement of a K x-ray isotope shift was carried out in our laboratory in 1965. In this experiment, Brockmeier *et al.*¹ used a curved-crystal spectrometer in the DuMond geometry to measure the $\text{U}^{233,238}$ $K\alpha_1$ x-ray isotope shift. Subsequent measurements by Sumbaev and Mezentsev² demonstrated the superiority of the curved-crystal spectrometer in the Cauchois geometry for x-ray shift measurements. We report here the results of x-ray shift measurements for a number of elements using the Cauchois geometry. The results for Sn, Sm, and W have been reported earlier.³

2. THEORY

The isotope shifts have been attributed to two effects. The first concerns the changes in the nuclear charge distribution (volume effect); the second has to do with the change in the center-of-mass motion of the nucleus.

* This work was performed under the auspices of the U. S. Atomic Energy Commission. Prepared under Contract AT(04-3)-63 for the San Francisco Operations Office, U. S. Atomic Energy Commission.

¹ R. T. Brockmeier, F. Boehm, and E. N. Hatch, *Phys. Rev. Letters* **15**, 132 (1965).

² O. I. Sumbaev and A. F. Mezentsev, *Zh. Eksperim. i Teor. Fiz.* **49**, 459 (1965) [English transl.: *Soviet Phys.—JETP* **22**, 323 (1966)].

³ R. B. Chesler, F. Boehm, and R. T. Brockmeier, *Phys. Rev. Letters* **18**, 953 (1967); F. Boehm and R. B. Chesler, in *Proceedings of the International Conference on Nuclear Structure, Tokyo, 1967* (Physical Society of Japan, to be published).

The largest contribution to the isotope shifts for atomic number $Z \gtrsim 30$ stems from the volume effect. The volume effect is due mainly to the change in the electric monopole interaction between the nucleus and the atomic electrons. A similar contribution, of the order of 2% or less, arises from the effects of mutual dynamic quadrupole polarization of the nucleus and the atomic electrons. In order to extract the nuclear charge radius from the isotope shift data, the mass shift was first subtracted from the observed shift. The resultant shift $\delta(\Delta E)_{\text{exp}}$ was compared to a standard theoretical shift $\delta(\Delta E)_{\text{std}}$ which takes into account the electric monopole interaction with an electrodynamic correction, and the dynamic quadrupole interaction.

It has been customary to compare the measured shift with the calculated standard shift of the mean-square charge radius, assuming a nuclear volume change obeying the $A^{1/3}$ law. Although the $A^{1/3}$ law poorly represents the experimental findings of optical and muonic shifts, we adopt this convention for our purpose, its main virtue being the possibility of easily comparing results from different experiments.

Calculations of the volume effect shifts of $K\alpha_1$ x rays have been carried out by Babushkin.⁴ These calculations are based on the nonperturbation method introduced by Broch.⁵ It has been demonstrated by Bodmer⁶ and later by Fradkin⁷ that the shifts depend only on the changes in the rms charge radius. Using the equivalent (uniform distribution) radius $R = (5/3)^{1/2} R_{\text{rms}}$ of a nuclear charge distribution with rms-radius R_{rms} , the volume shift is proportional to $\delta R / \bar{R}$, where for a pair of isotopes \bar{R} and δR are the mean value and the change, respectively, of the equivalent radius. The volume shifts $\delta(\Delta E)_B$ calculated by Babushkin for an equivalent charge radius dependence of $1.2 \times 10^{-13} A^{1/3}$ cm are given in column 2 of Table I. For the $K\alpha_1$ transition, the harder x ray belongs to the lighter isotope.

⁴ F. A. Babushkin, *Opt. i Spektroskopiya* **15**, 721 (1963) [English transl.: *Opt. Spectry. (USSR)* **15**, 393 (1963)].

⁵ E. K. Broch, *Archiv Math. Naturvid.* **48**, 25 (1945).

⁶ A. R. Bodmer, *Nucl. Phys.* **9**, 371 (1958-59).

⁷ E. E. Fradkin, *Fiz.* **42**, 787 (1962) [English transl.: *Soviet Phys.—JETP* **15**, 550 (1962)].

TABLE I. Calculated $K\alpha_1$ isotope shifts.

1	2	3	4		5	
Isotope pair	$\delta(\Delta E)_B$ (meV)	Nontransition electron contribution	Correction factors		Dynamic nuclear polarization	$\delta(\Delta E)_{\text{std}}$ (meV)
			Electro- dynamic correction			
Sn 116-124	76.9	0.96	0.944		1.00	69.7
Nd 144-150	147.3	0.97	0.945		0.98	132.7
Sm 148-154	177.0	0.97	0.942		0.98	158.7
Gd 155-156	35.3	0.97	0.943		0.974	31.4
156-160	140.2	0.97	0.943		0.987	126.6
155-160	175.5	0.97	0.943		0.983	157.8
W 182-184	152	0.98	0.937		1.016	141.8
184-186	151	0.98	0.937		1.004	139.2
182-186	303	0.98	0.937		1.010	280.9
Hg 200-204	551	0.98	0.938		1.014	513.6
Pb 206-208	326	0.98	0.937		1.003	300.2

The values $\delta(\Delta E)_B$ take account of the screening of the transition electron by the other atomic electrons by the method of Slater's rule.⁸ However, the contribution to the isotope shift of the nontransition atomic electrons is not included in $\delta(\Delta E)_B$. This contribution arises from the changed screening effect of the transition electron on the other atomic electrons in its initial (L_{III}) and final (K) states. Estimates of this effect have been given by Wertheim and Igo⁹ for transitions in Mo and U. In column 3 of Table I similar corrections have been determined as factors to be applied to $\delta(\Delta E)_B$.

An electrodynamic modification of the ordinary volume effect worked out by Breit and Clendenin¹⁰ has been included in the present analysis. By considering the radiative correction to the electron magnetic moment in the presence of the nuclear electric field, the ordinary volume effect included in $\delta(\Delta E)_B$ is decreased by the factor

$$1 - \frac{Z\alpha(2\rho+1)(2\rho+3)}{8\pi r_0(\rho+1)}, \quad (1)$$

where $\rho = [1 - (Z\alpha)^2]^{1/2}$ and r_0 is the nuclear radius ($1.2 \times 10^{-13} A^{1/3}$ cm) in units of e^2/mc^2 . The correction factors to $\delta(\Delta E)_B$ are given in column 4 of Table I.

In strongly deformed nuclei there is a dynamical quadrupole interaction between the nucleus and the atomic electrons. Reiner and Wilets¹¹ have calculated the associated energy shift by using second-order perturbation theory. Assuming the rotational model applies, the diagonal quadrupole moment is proportional to the deformation parameter β , and a second-order calculation results in a shift $\delta(\Delta E)_{\text{dynamic}}$ proportional to $\delta(\beta^2)$. The static effect of the deformation is

given⁷ approximately by

$$\delta(\Delta E)_{\text{static}} \approx \delta(\Delta E)_B (5/8\pi) \delta(\beta^2) (3\bar{A}/\delta A), \quad (2)$$

where $\delta(\beta^2)$ is the difference in the square of the deformation parameter β^2 between the isotopes, and \bar{A} and δA are the mean value and isotopic change of the mass number. For the purposes of calculating the small dynamic quadrupole correction, we have neglected in Eq. (2) the effects of higher-order terms and radial and deformation nuclear compressibilities. Since both $\delta(\Delta E)_{\text{static}}$ and $\delta(\Delta E)_{\text{dynamic}}$ are proportional to $\delta(\beta^2)$, Reiner and Wilets have expressed their result as a ratio of the two effects,

$$\delta(\Delta E)_{\text{dynamic}}/\delta(\Delta E)_{\text{static}} = -Z\alpha/4\pi, \quad (3)$$

which indicates that the polarization shift decreases the deformation contribution to the isotope shift by a few percent. Using the intrinsic deformations listed by Stacey¹² and Eq. (2) for the static quadrupole contribution, we derive the correction factors to $\delta(\Delta E)_B$ appearing in column 5 of Table I. In column 6 are the resultant "standard shifts" $\delta(\Delta E)_{\text{std}}$ expected for the equivalent charge radius dependence $R = 1.2 \times 10^{-13} A^{1/3}$ cm.

It should be noted that $\delta(\Delta E)_{\text{std}}$ depends on the static deformation change only through the higher-order correction (3). A first-order static deformation correction as quoted in Refs. 4 and 7 has not been included.

The mass shift arises from a variation in the recoil energy of the nucleus from one isotope to another. In the c.m. system of an atom, the total kinetic energy T is approximated by the nonrelativistic expression

$$T = \sum_{i=1}^Z \frac{\mathbf{P}_i^2}{2m} + \left(\sum_{i=1}^Z \mathbf{P}_i \right)^2 / 2M,$$

where \mathbf{P}_i is the momentum of the i th electron, m is the electron mass, and M is the nuclear mass. Singling out

⁸ J. C. Slater, Phys. Rev. **36**, 57 (1930).

⁹ M. S. Wertheim and G. Igo, Phys. Rev. **98**, 1 (1955).

¹⁰ G. Breit and W. W. Clendenin, Phys. Rev. **85**, 689 (1952); G. Breit, Rev. Mod. Phys. **30**, 507 (1958).

¹¹ A. S. Reiner and L. Wilets, Nucl. Phys. **36**, 457 (1962).

¹² D. N. Stacey, Rept. Progr. Phys. **29**, 171 (1966).

the cross term and combining the square terms gives

$$T = \sum_{i=1}^Z \frac{\mathbf{P}_i^2}{2\mu} + \sum_{i>j=1}^Z \frac{\mathbf{P}_i \cdot \mathbf{P}_j}{M},$$

where

$$\mu = [mM/(m+M)] \quad (4)$$

is the reduced electron mass. To the extent that spin-orbit forces are negligible in comparison to Coulomb forces, the reduced-mass term above results in a linear contraction of the atomic spectrum of the form $E(\mu) = (\mu/m)E(m)$ as shown, for example, by Huges and Eckart.¹³ The cross term above gives rise to the specific mass shift. Its effect has been calculated as a first-order perturbation in the present work for the $K\alpha_1$ transition for $Z=42, 50, 62,$ and 74 using the radial functions calculated by Herman and Skillman.¹⁴ Because we deal with closed-shell or single-hole configurations in the x-ray case, configuration mixing does not occur and the perturbation calculation is straightforward. Higher-order relativistic corrections to the perturbing operator are negligible because of the large nuclear mass. The details of the method of calculation are similar to those of an earlier specific mass shift calculation by Vinti.¹⁵ The present calculations show that the $K\alpha_1$ mass shift

depends essentially on the core electrons, and therefore varies smoothly with atomic number. In particular, the specific shift was found to be numerically equal to $\approx -\frac{1}{3}$ times the normal reduced-mass shift for $40 \leq Z \leq 74$. The total mass shift $\delta(\Delta E)_M$ (normal+specific) of the $K\alpha_1$ x ray is therefore given by

$$\delta(\Delta E)_M \approx \frac{2}{3}(\delta A/1836\bar{A}^2)E_{K\alpha_1}, \quad (5)$$

where \bar{A} and δA are the average mass number and neutron difference, respectively, for the isotope pair, and $E_{K\alpha_1}$ is the $K\alpha_1$ x-ray energy.

The contribution of the Lamb shift of the K level¹⁶ to the isotope shift through its reduced-mass dependence has been found to be negligible.

3. EXPERIMENT

A bent-crystal diffraction spectrometer with 2 m radius of curvature described in detail by Seppi *et al.*¹⁷ was used for the present investigations. The spectrometer was set up in the Cauchois geometry, i.e., a detecting slit was located at the focal point of the bent (310) quartz crystal. The apparatus used to measure the x-ray shifts is pictured schematically in Fig. 1. The present method is in many respects similar to that employed

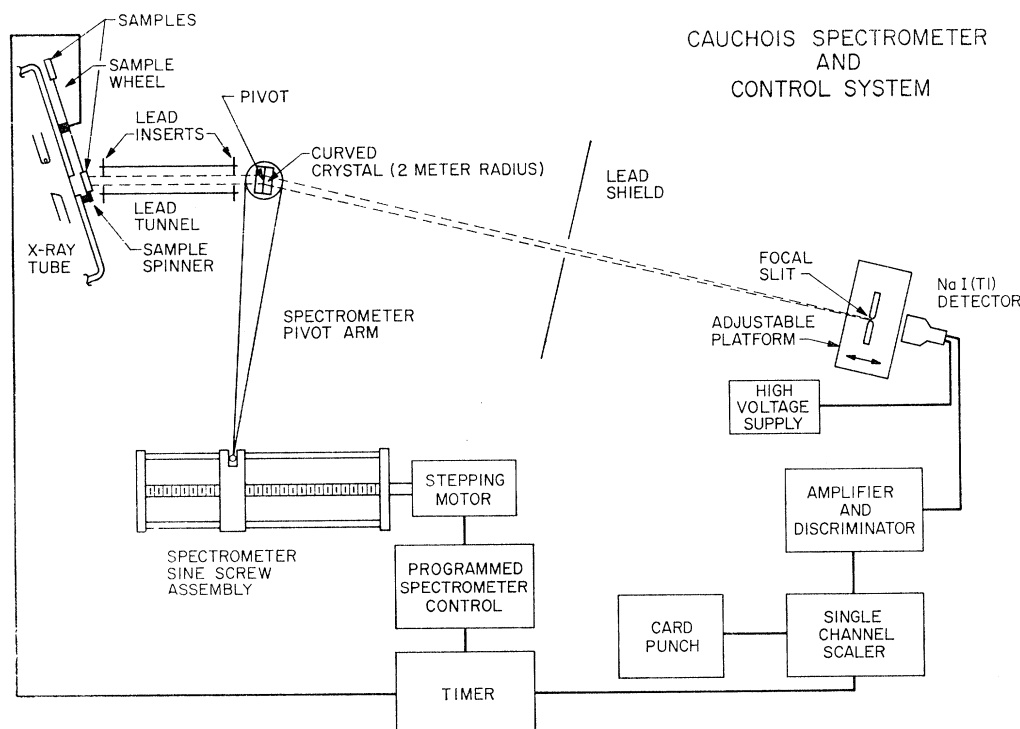


FIG. 1. Cauchois spectrometer and control system.

¹³ D. J. Huges and C. Eckart, *Phys. Rev.* **36**, 694 (1930).

¹⁴ F. Herman and S. Skillman, *Atomic Structure Calculations* (Prentice-Hall, Inc., Englewood Cliffs, N. J., 1963).

¹⁵ J. P. Vinti, *Phys. Rev.* **56**, 1120 (1939).

¹⁶ N. Kroll and W. Lamb, *Phys. Rev.* **75**, 388 (1949).

¹⁷ J. E. Seppi, H. Henrikson, F. Boehm, and J. W. M. DuMond, *Nucl. Instr. Methods* **16**, 17 (1962).

by Sumbaev and Mezentsev in connection with x-ray chemical shift¹⁸ and isotope shift experiments.^{2,19}

Each measurement involved the comparison of a pair of isotopically enriched samples of similar crystalline structure. The isotopes were obtained from the Oak Ridge National Laboratory in quantities of about 1 g. Table II gives the chemical forms and enrichments of the samples studied as well as the $K\alpha_1$ wavelengths and energies.²⁰ Since the x-ray energy is dependent on the chemical form, it is imperative that the samples to be compared have the same chemical form and crystallographic structure. High-resolution powder pictures of the samples obtained with a Guinier camera were analyzed to determine the crystalline structures and to detect possible mixtures and impurities to concentrations down to 0.25%. Dissimilar structures were found for the cases of Sm_2O_3 and Nd_2O_3 . In these cases it was necessary to modify the original crystalline mixtures by

TABLE II. Chemical form, isotopic enrichment, and $K\alpha_1$ wavelengths and energies.

Sample	Chemical form	Isotopic enrichment (%)	$\lambda(K\alpha_1)$ (xu)	$E(K\alpha_1)$ (keV)
Sn 116	SnO ₂	95.60	490.599	25.2713
124		94.74		
Nd 144	Nd ₂ O ₃	94.4	331.846	37.3610
150		95.98		
Sm 148	Sm ₂ O ₃	95.37	309.040	40.1181
154		99.30		
Gd 155	Gd ₂ O ₃	94.4	288.353	42.9962
156		99.82		
160	WO ₃	95.2	209.010	59.3182
W 182		94.32		
184		94.22		
186		97.06		
Hg 200	HgO	88.92	175.068	70.819
204		64.2		
Pb 206	Pb(NO ₃) ₂	97.39	165.376	74.969
208		97.98		

roasting in air at 1300°C to bring the samples to a common structure.²¹ Taking a typical value of 100 meV for an x-ray chemical shift as measured in our laboratory²² as an estimate of the shift to be expected from structural difference, the quoted degree of uniformity of the sample ensured that such structural shifts could be neglected in comparison to other sources of experimental error.

The powdered samples were loaded into cylindrically shaped Lucite holders carefully machined to the optimum cavity thickness. The optimum thickness was determined empirically by studying the fluorescent

¹⁸ O. I. Sumbaev and A. F. Mezentsev, Zh. Eksperim. i Teor. Fiz. 48, 445 (1965) [English transl.:—JETP 21, 295 (1965)].

¹⁹ O. I. Sumbaev *et al.*, Yadern. Fiz. 5, 544 (1967) [English transl.: Soviet J. Nucl. Phys. 9, 15 (1967)].

²⁰ J. A. Bearden, Rev. Mod. Phys. 39, 78 (1967).

²¹ C. E. Curtis and J. R. Johnson, J. Am. Ceram. Soc. 40, 15 (1957).

²² B. G. Gokhale, R. B. Chesler, and F. Boehm, Phys. Rev. Letters 18, 957 (1967).

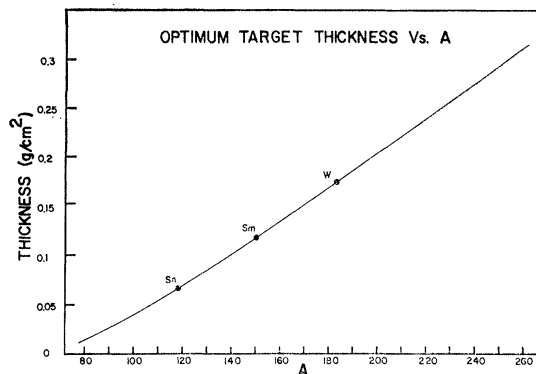


Fig. 2. Optimum target thickness versus atomic number A .

intensity as a function of target thickness. It corresponds to the point of maximum intensity ($dI/dx=0$). Figure 2 shows a plot of optimum thickness versus mass number A for elements of natural isotopic composition. The holders were mounted on a rotatable wheel (Fig. 1) permitting the exposure of the samples alternately to the bremsstrahlung beam of a 150-kV, 20-mA x-ray tube. During exposure each sample was spun about its center to reduce aberrational errors from inhomogeneous aximuthal source distributions.

The $K\alpha_1$ fluorescence x rays of the sample were analyzed by the curved-crystal Cauchois spectrometer. The spectrometer quartz crystal had a diffraction width of 0.22 xu (19 sec of arc). In comparison to that the natural x-ray widths varied from 0.13 to 0.23 xu for the elements investigated. The lead alloy slit located at the spectrometer focus had a width equal to the combined instrumental and natural widths. A NaI(Tl) detector was located behind the slit.

The lead tunnel shown in Fig. 1 served to absorb the direct bremsstrahlung beam. The lead insert shown closest to the sample had a circular aperture of 2.3 cm, slightly smaller than the size of the sample, therefore ensuring that the source area for the spectrometer did not vary in position as a result of slight variations in the resting position of the sample wheel.

The $K\alpha_1$ line was scanned repetitively in 35 angular steps by means of the stepping motor connected to the precision sine screw which rotates the crystal. For the small range of scan (~ 2 min of arc) it was not necessary to also move the target. The two samples were placed alternately in the bremsstrahlung beam at each step of the scan in order to minimize errors due to apparatus drift. Each counting period was 20 sec, and the dead time during sample interchange was about 5 sec. With this arrangement drift errors were less than half the size of the uncertainties due to counting statistics. Peak counting rates varied from 400/sec to 2000/sec and each experiment lasted from 1 to 2 weeks.

Least-squares fits were made by computer to the line profiles corresponding to each sample. Data from four scans across the $K\alpha_1$ profile were summed for each least-

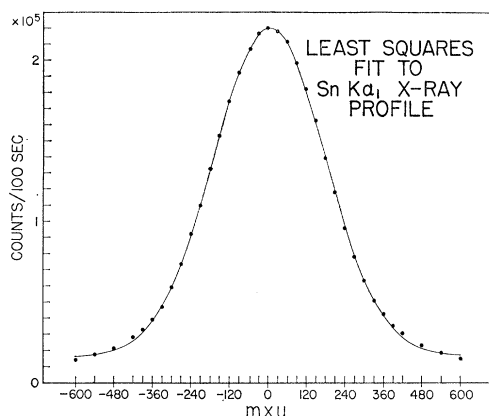


FIG. 3. Typical Sn $K\alpha_1$ x-ray profile and least-squares fit.

squares fit. The data for each experiment comprised 50 or more such fits, and the assigned error is derived from the statistical fluctuation of these individual values. A typical data profile and fitting function are shown in Fig. 3. A five-parameter fit function was used consisting of a Gaussian plus two parameters for the average value and slope of the background. Small systematic differences between the profile shape and the fitting function are of no concern in the present comparison provided the profiles of the compared samples are sufficiently alike. This point will be discussed below in connection with the effects of instrumental aberrations.

Ideally, the line profile produced by the Cauchois spectrometer is invariant with respect to small displacement of the source. In practice, however, profile shifts of the order of 0.01 xu may be produced by placing a relatively small source in various positions with respect to the crystal. Such aberrations result from imperfections in the quartz crystal structure and bending and from the vertical divergence effect which contributes about 0.006 xu variation according to the formula

$$\Delta\lambda \cong \lambda s^2 / 8a^2, \quad (6)$$

where s is the slit height and a is the crystal-to-slit distance. Aberrational shifts may be produced not only by varying the position of a small sample but also by varying the intensity distribution across the surface of extended samples, such as were employed in the present experiments. Although spinning the samples eliminated azimuthal variations, radial variations remained. The observed profile may then be considered to be a weighted integral of the constituent profiles from different parts of the curved crystal, the weights being in proportion to the fluorescence luminosity of the corresponding part of the sample.

Direct measurements of aberrational shifts using two samples of isotopically natural H_2WO_4 arranged as in the actual shift measurements yielded a shift of 0.00 ± 0.04 mxu. This uncertainty is of the same approximate size as those in the actual shift measurements. A second experimental method was employed to more closely determine the magnitude of the aberrational shifts. Two isotopically natural H_2WO_4 samples were prepared, each of only $\frac{1}{2}$ the optimum thickness used for the shift experiments. Because the aberrational shifts depend on the variations in intensity across the surfaces of the extended samples, such shifts are exaggerated by the samples of half-optimum thickness for a given variation in sample thickness. The samples used in the isotope shift experiments were prepared with sufficient care to ensure their being within 5% of the optimum mass thickness. Assuming the maximum 5% error in mass thickness we estimate from a plot of intensity versus thickness that aberrations are decreased by a factor of ≈ 6.5 when compared to those associated with the half-optimum-thickness sources. The shift measured between the isotopically natural wolfram samples of half-optimum thickness was 0.04 ± 0.05 mxu. This leads to an uncertainty of ≈ 0.01 mxu for optimum thickness targets. This may be compared to a typical uncertainty from counting statistics of ± 0.03 mxu. Other aberrational effects such as those associated with the slight variation of the x-ray absorption coefficients over the x-ray linewidth are negligible. The careful preparation

TABLE III. Experimental $K\alpha_1$ x-ray isotope shifts.

Isotope pair	Uncorrected shifts		Corrected shifts (meV)	Volume shifts $\delta(\Delta E)_{exp}$ (meV)	$\frac{\delta(\Delta E)_{exp}}{\delta(\Delta E)_{std}}$
	(mxu)	(meV)			
Sn 116-124	0.560 ± 0.020	28.8 ± 1.0	29.9 ± 1.2	35.0 ± 1.3	0.50 ± 0.02
Nd 144-150	1.823 ± 0.027	205.3 ± 3.0	216.8 ± 3.5	220.7 ± 3.5	1.66 ± 0.04
Sm 148-154	2.059 ± 0.023	267.3 ± 3.0	271.6 ± 3.5	275.5 ± 3.5	1.74 ± 0.04
Gd 155-156	0.183 ± 0.047	27.3 ± 7.0	33.6 ± 5.4	34.3 ± 5.4	1.09 ± 0.17
156-160	0.636 ± 0.036	94.8 ± 5.4	100.0 ± 4.6	102.5 ± 4.6	0.81 ± 0.04
155-160	0.864 ± 0.031	128.8 ± 4.6	133.6 ± 4.2	136.8 ± 4.2	0.87 ± 0.03
W 182-184	0.281 ± 0.038	79.8 ± 10.8	90.9 ± 10.5	92 ± 10.5	0.65 ± 0.08
184-186	0.188 ± 0.029	53.4 ± 8.2	58.5 ± 8.0	60 ± 8	0.43 ± 0.06
182-186	0.477 ± 0.035	135.4 ± 10.0	149.4 ± 10.0	152 ± 10	0.54 ± 0.04
Hg 200-204	0.416 ± 0.061	168 ± 25	252 ± 37	254 ± 37	0.49 ± 0.07
Pb 206-208	0.351 ± 0.053	159 ± 24	166 ± 25	167 ± 25	0.56 ± 0.08

of the optimum-thickness samples thus guarantees sufficient similarity in the compared profile shapes to avoid systematic error greater than ± 0.01 mxu.

4. RESULTS

Table III gives the present experimental results. The uncorrected shifts are presented in wavelength units in column 2. The uncertainties are derived from the spread of individual shift values about the mean. Column 3 gives the same shifts in energy units. In all cases presented here, the sign of the shift corresponds to a nuclear charge radius increasing with neutron number. The following modifications of the values of column 3 yield the corrected shifts of column 4: In the cases of W, an empirically determined 5.8% correction for the elastic scattering of characteristic $K\alpha_1$ radiation of the W anode of the x-ray tube has been applied. For the Gd and W measurements a consistency constraint has been applied which requires that the sum of the smaller neutron shifts measured equal the larger neutron shift, with an accompanying small decrease in the resultant uncertainties. In all cases, a correction for the isotopic enrichment of the samples has been applied, evaluated by the use of relative optical data. In addition, the uncertainty ± 0.01 mxu ascribed to aberrations has been taken into account in column 4.

In column 5 appear the experimental volume shifts $\delta(\Delta E)_{\text{exp}}$ obtained from the values of column 4 by subtracting the total mass shifts given by Eq. (5). In column 6 is the ratio $\delta(\Delta E)_{\text{exp}}/\delta(\Delta E)_{\text{std}}$ of the experimental volume shifts to the calculated shifts (Table I, column 6) for equivalent radii given by $R=1.2 \times 10^{-13} A^{1/3}$ cm. This ratio corresponds to the relative change in equivalent radius, $\delta R/R$, in units of $\delta A/3A$. The uncertainties in column 6 take into account $\pm 2\%$ for the calculated values $\delta(\Delta E)_{\text{std}}$.

5. DISCUSSION

The optical¹² and muonic x-ray²³ two-neutron isotope shift data for even neutron numbers in Sn, Nd, Sm, Gd, W, Hg, and Pb are plotted in Fig. 4 versus the larger neutron number of the pair. For W and Pb, the present x-ray results also are presented. In the other cases where the present work does not supply two-neutron shifts we have compared our results to the optical data as follows. Revised optical shifts were obtained by adding a constant to each optical two-neutron shift in a given elemental group to bring them into agreement with the present multiple-neutron results. This revision in fact corresponds to a determination of the unknown optical specific mass correction. Because of the additional large uncertainty of the screening correction factor to the electron density change at the nucleus in the optical case, the revision

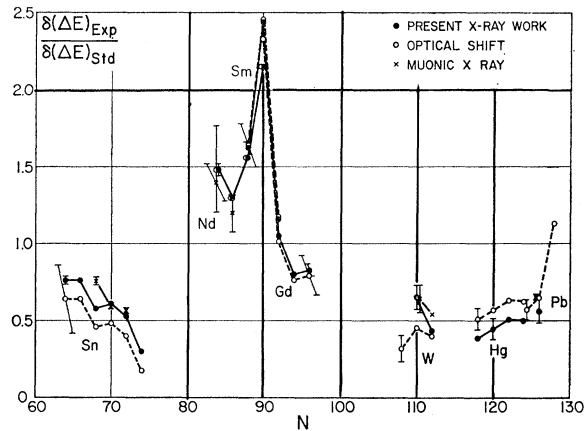


FIG. 4. Brix-Kopfermann diagram of experimental results. The two-neutron isotope shifts versus the neutron number of the heavier isotope are presented for the optical and muonic data for Sn, Nd, Sm, Gd, W, Hg, and Pb along with the present x-ray results. Absolute two-neutron x-ray shifts are shown for W and Pb. For the other elements, where two-neutron shifts have not been measured in the present experiments, renormalizations of the optical data by the present x-ray results are given.

adopted is somewhat arbitrary but would appear to represent the best approach to combining the absolute x-ray shifts with the optical data at present. The present x-ray measurement applied to the optical shift data of Stacey²⁴ fixes the specific mass shift of λ 3283 Å in Sn II at the value -2.6 mK per neutron. The value earlier used by Stacey²⁴ of -4 mK was little more than an order-of-magnitude estimate. The present value agrees very well with a determination of the same quantity based on muonic x-ray shifts.²⁵ In the cases of Nd, Sm, and Gd, Fig. 4 shows that the present results indicate no significant error in the optical specific mass shift estimates. For heavier elements the determination of the optical mass shift becomes impractical because of the greater relative importance of optical screening corrections.

A direct comparison with the Nd¹⁴⁴⁻¹⁵⁰ $K\alpha_1$ x-ray shift measured by Sumbaev *et al.*¹⁹ can be made. Their value, corrected for the specific mass shift, of (237 ± 13) meV is consistent with the present result of (220.7 ± 3.5) meV. The comparison of Ref. 3 between our Sm¹⁴⁸⁻¹⁵⁴ measurement and those of Sumbaev *et al.*¹⁹ in Sm¹⁴⁴⁻¹⁵⁰ and Sm¹⁴⁴⁻¹⁵² through the use of relative optical shift data also yielded satisfactory agreement.

The experimental data from K x rays, optical lines, and muonic x rays are in good agreement except perhaps in the cases of the relative shifts in Sn and W. Further measurements of these shifts would be useful. The general agreement among the various data supports the accuracy of the coupling calculations involved in each of the three branches of experimentation. The

²³ R. D. Ehrlich *et al.*, Phys. Rev. Letters **18**, 959 (1967); Phys. Letters **23**, 468 (1966); T. T. Bardin *et al.*, Phys. Rev. Letters **16**, 718 (1966).

²⁴ D. N. Stacey, Proc. Roy. Soc. (London) **A280**, 439 (1964).

²⁵ R. D. Ehrlich (private communication).

large anomalies of the isotope shift reported early from the optical work²⁶ and more recently by the muonic work²³ are established with good accuracy by the present results. It appears evident that the $A^{1/3}$ law or its refinements are unable to reproduce the detailed variations in the observed shifts. Calculation of the isotope shift based on microscopic models²⁷⁻²⁹ have been only partially successful in explaining the observations. In the case of light nuclei a more successful treatment

was proposed by Perey and Schiffer.³⁰ Further theoretical work, particularly in the case of heavy nuclei, seems desirable.

ACKNOWLEDGMENTS

The authors would like to acknowledge the help of Dr. S. Samson in the crystallographic analysis and are grateful to Professor P. Duwez for his aid in carrying out crystal-structure modifications. Particular thanks are due to Professor B. G. Gokhale for valuable discussions, to P. Lee for helping with the experiments, and to H. Henrikson for designing the curved-crystal spectrometer.

²⁶ P. Brix and H. Kopfermann, *Rev. Mod. Phys.* **30**, 517 (1958).

²⁷ R. A. Uher and R. A. Sorensen, *Nucl. Phys.* **86**, 1 (1966).

²⁸ G. G. Bunatyan and M. A. Mikulinsky, *J. Nucl. Phys. (USSR)* **1**, 38 (1965).

²⁹ V. P. Kraynov and M. A. Mikulinsky, *J. Nucl. Phys. (USSR)* **4**, 928 (1966).

³⁰ F. G. Perey and J. P. Schiffer, *Phys. Rev. Letters* **17**, 324 (1966).

Decay Scheme of $^{158}\text{Tb}^\dagger$

D. SCHROEER* AND P. S. JASTRAM
Ohio State University, Columbus, Ohio

(Received 21 April 1967; revised manuscript received 16 October 1967)

A study has been made of the decay of ^{158}Tb , including measurements of transition intensities, lifetimes of excited states, and angular correlations. The resulting decay scheme is generally in agreement with that proposed in previous studies. Major modifications include a new level at 819 keV in ^{158}Dy , and several new γ -ray transitions which were seen in coincidence studies and which may be due to a long-lived isomeric state in ^{158}Tb . Also, improvement was attained in the precision of the intensities of several weak γ -ray transitions, and of the β -branching ratio. The lifetimes of the first 2^+ states in ^{158}Gd and ^{158}Dy were re-determined for several different cascades through β - γ as well as γ - γ coincidence-delay studies; the values measured were, respectively, 2.59 ± 0.10 and 1.76 ± 0.10 nsec. The 1188-keV state and the 1107-keV γ -ray transition in the decay to ^{158}Gd were confirmed to be, respectively, a 2^+ state and an $E2$ transition through an angular-correlation measurement. These modifications and improvements in the decay scheme are discussed on the basis of the rotational model of deformed nuclei.

1. INTRODUCTION

THE decay of ^{158}Tb , via β decay to ^{158}Dy and via electron capture to ^{158}Gd , is significant because both of the daughter nuclei are links in chains of fairly extensively investigated even-even nuclei with 64 and 66 protons, respectively, just inside the region of permanently deformed nuclei. Comparison of the changes of the levels of these nuclei with decreasing neutron number will, hopefully, help in improving our understanding of the effects of changing deformation and decreasing neutron number.

The basic decay scheme of ^{158}Tb has been established primarily through a conversion-electron and β -decay study by Naumann, Nielsen, and Skilbreid,¹ and

through a more recent study of the γ -ray and electron spectra by Schima, Funk, and Mihelich.² Their results are consistent with the modified decay scheme proposed in the present work (Fig. 1). Reference 3 summarizes the earlier studies of the ^{158}Tb decay, as well as investigations of the decay of ^{158}Eu and ^{158}Ho to levels in ^{158}Gd and ^{158}Dy , and of Coulomb-excitation results for these isotopes.

The present work presents a reinvestigation of the decay of ^{158}Tb , using a chemically and isotopically separated source. After production in the ARCO reactor, and chemical separation by Dr. R. A. Naumann of Princeton University, the source was deposited as a line 1.5 mm wide by 12 mm long on aluminum of about 100 g/cm² thickness in the Copenhagen isotopic separator. This reinvestigation includes electron and γ -ray

[†] Supported in part by the U. S. Atomic Energy Commission. Based on a thesis submitted by one of the authors (D. S.) to the Ohio State University in partial fulfillment of requirements for the Ph.D. degree.

* Present address: Department of Physics, University of North Carolina, Chapel Hill, N. C.

¹ R. A. Naumann, O. B. Nielsen, and O. Skilbreid, *Bull. Am. Phys. Soc.* **7**, 34 (1962).

² F. Schima, E. G. Funk, Jr., and J. W. Mihelich, *Nucl. Phys.* **63**, 305 (1965).

³ *Nuclear Data Sheets*, compiled by K. Way *et al.* (Printing and Publishing Office, National Academy of Science—National Research Council, Washington 25, D. C., 1964).